Int. J. Electrochem. Sci., 15 **(2020)** 8960 – 8970, doi: 10.20964/2020.09.03

International Journal of
ELECTROCHEMICAL
SCIENCE
www.electrochemsci.org

Characterization and Analysis of Chromium Coating Electrodeposited on Brass in ChCl-EG Deep Eutectic Solvent

Huixuan Qian, Qisong Li, Jie Sun[*], *Souavang Xaikoua, Haijing Sun*

School of Environmental and Chemical Engineering, Shenyang Ligong University, Shenyang, 110168, P. R. China
[*]E-mail: jiersun2000@126.com

Received: 16 March 2020 / *Accepted:* 10 June 2020 / *Published:* 10 August 2020

Black chromium coating was electrodeposited on brass substrate from choline chloride-ethylene glycol (ChCl-EG) deep eutectic solvent (DES), via potentiostatic electrodeposition method. Cyclic voltammetry method was used to study the electrochemical reduction behavior of trivalent chromium ions (Cr^{3+}) in ChCl-EG deep eutectic solvent. The composition and morphology of coating were characterized by X-ray photoelectron spectroscopy and scanning electron microscopy. The results showed that the electrochemical reduction of Cr(III) followed a two-step process, Cr(III) to Cr(II), and Cr(II) to Cr(0). Furthermore, the results indicated the existence of Cr and O elements in the coating, which was composed of chromium oxide, chromium hydroxide, and metallic chromium. Formation of the mixed phase was primarily caused by water molecules existing in the ChCl-EG deep eutectic solvent.

Keywords: Deep eutectic solvent; Chromium; Electrodeposition; Electrochemical reduction behavior; Morphology

1. INTRODUCTION

Chromium coating is widely used in surface modification, decorative materials, anti-wear materials, and anti-corrosion materials, due to its excellent properties including corrosion and wear resistance [1]. Currently, the development of chromium electrodeposition process using hexavalent chromium (Cr(VI)) electrolyte is very mature. However, high toxicity and strong carcinogenicity of Cr(VI) ions in traditional chromate solution seriously impact the environment and human health. Although Cr(VI) is ubiquitous in its use for corrosion protection, countries around the world have imposed legal restrictions on the use of Cr(VI) and it is expected that there will be other restrictions in future [2]. Under this circumstance, electrodeposition of chromium from an aqueous solution of trivalent chromium (Cr(III)) ions with lower toxicity has attracted significant attention of researchers and related in-depth research has been conducted.

Since the beginning of the Cr(III) electrodeposition studies in the United States in 1976, they have been fully developed [3,4]. In general, Cr(III) is mainly present in aqueous solution in the form of $[Cr(H_2O)_6]^{3+}$ with a regular octahedral structure, and its stability is not conducive to the contact of cathode electrons with Cr^{3+} center [2]. Notably, the high stability of the regular octahedral structure directly hinders the electrodeposition of chromium [5]. In order to solve this problem, a series of additives such as formic acid, acetic acid, glycine, and other organic additives has been introduced to replace the water molecules present in the inner sphere of $[Cr(H_2O)_6]^{3+}$ [5–7]. The results indicate that the introduction of the ligands mentioned above can change the structure of $[Cr(H_2O)_6]^{3+}$, making it no longer have a symmetrical octahedral structure. Moreover, the ligand field splitting energy is reduced and the kinetic stability is also reduced, which is beneficial to the reduction of Cr(III) on the cathode surface. However, introduction of these additives still leads to the following problems: (1) difficulty to obtain a thick and high-quality coating; (2) narrow working pH range; (3) high susceptibility of electrolyte to impurities, and (4) difficulty to store and reuse the electrolyte.

In recent years, ionic liquids (IL) have attracted extensive research attention due to their unique physical properties (low melting point, low vapor pressure, high polarity range, high thermal stability, and good solvent properties, etc.) and low toxicity in the field of electrodeposition [8–10]. In these researches, the researchers mainly investigated the mixing of metal salts (mainly salts of zinc, aluminum, tin, and iron) with quaternary ammonium salts to form ILs [10]. Subsequently, the choline-based raw materials were confirmed to be suitable for the formation of room temperature ionic liquid (RTIL) [11,12]. Researchers believe that RTILs exhibit the potential for large-scale applications, such as electrodeposition, batteries [13], and catalysis [14]. The formation of a new generation IL usually involves the combination of choline chloride (ChCl) and hydrogen bond donors (HBDs) (e.g. urea, renewable carboxylic acids, etc.). Compared to the traditional ILs, the ChCl-based DES has the following advantageous characteristics: (1) cost effective; (2) easy to store; (3) easy to prepare (by simple mixing of components); and (4) biodegradable and biocompatible [15]. Noteworthy, the freezing point of the ChCl-HBD IL is generally lower than that of each component due to the interaction between the halide anion and the HBD component. Moreover, the organic salt/HBD molar ratio also significantly affects the freezing point of the IL. For example, when the molar ratio of ChCl to urea is 1:1 and 1:2, the solidification points of IL are >50 °C and 12 °C, respectively [9,14,15].

In order to study the application of ILs to electrodeposition of chromium, electrodeposition of Cr(III) was studied in $[BMIm][BF_4]$ [16], [BMIm]Br [17], $[BMIm]HSO_4$ [18], ChCl-EG [19], and Type-4 RTIL [10]. In these studies, the in-depth research was carried out on the electrochemical behavior, nucleation, and growth mechanisms [19,20]. The effects of temperature on electrodeposition rate, coating thickness, and corrosion resistance were also systematically analyzed. Noteworthy, the chromium coating obtained via electrodeposition method in different ILs are usually non-metallic bright. For example, Survilienė et al. [16] and Eugénioa et al. [21] electrodeposited a black chromium coating from $[BMIm][BF_4]$ solution consisting of a mixture of chromium oxide/hydroxide and metallic chromium [16,21]. Further, the black chromium layer with an amorphous submicron particle structure was obtained. He et al. also prepared a spherical and micron-grade black chromium coating from [BMIm]Br on Cu substrate [17]. He et al. also electrodeposited a nano-chromium coating in a $[BMIm]HSO_4$ IL, and the coating consisted of nanocrystalline chromium with a spherical structure

[18]. Abbott et al. electrodeposited pale blue/gray amorphous chromium coating from ChCl-$CrCl_3 \cdot 6H_2O$ DES and added Lithium chloride (LiCl) to the IL to obtain a nanocrystalline black chromium coating [22]. Nonetheless, in these studies, the discussion about the composition of coating and the reasons for its formation was limited.

In this study, the electrodeposition of chromium was carried out in ChCl-EG deep eutectic solvent. The electrochemical reduction behaviors of Cr(III) ions in ChCl-EG DES, phase composition, and morphology of chromium coating were analyzed by cyclic voltammetry (CV), X-ray photoelectron spectroscopy (XPS) and scanning electron microscopy (SEM) equipped with energy dispersive X-ray spectroscopy (EDS) system.

2. EXPERIMENTAL

The electrochemical method cyclic voltammetry (CV) was carried out to study the electrochemical behaviors of Cr(III) ions using CS350 electrochemical workstation at 333 K. The potentiostatic method (−1.35 V vs Pt) was used to perform the chromium electroplating for 30 min under stagnant conditions. The brass sheets were used as the substrate in electrodeposition. They were polished using up to 2000# grit sandpaper, and degreased with acetone, thoroughly washed with absolute ethanol and deionized water successively, and dried for future use.

In the experiment, a traditional three-electrode cell was used with glassy carbon (GC) electrode (3mm diameter, electrochemical reduction experiment) and brass sheet (electrodeposition) as the working electrode, Ag|AgCl electrode as the reference electrode, and Pt platinum electrode as the counter electrode. The scan rates of CV were 60 mV/s unless special description. Choline chloride ($C_5H_{14}ClNO$, 98%, ChCl), ethylene glycol ($C_2H_6O_2$, EG), and chromium chloride hexahydrate ($CrCl_3 \cdot 6H_2O$) were were analytical grade. ChCl and EG were mixed in a molar ratio of 1:1, 1:2, 1:3, and 1:4, respectively, and heated in a constant temperature oil bath at 333 K. Chromium chloride ($CrCl_3 \cdot 6H_2O$) was dissolved in ChCl-EG and stirred for 12 h to obtain ChCl-EG-Cr(III) electrolyte with concentration of 0.4 mol/L.

The micromorphology and elemental composition of coatings were characterized by SEM (VEGA3). The chemical composition and the state of elements were analyzed by XPS via Kratos-Axis Ultra System with monochromatic AlKα (1486.71 eV) X-ray radiation (15 kV and 10 mA) and hemispherical electron energy analyzer. The base vacuum of the chamber was 2×10^{-9} torr. The survey spectra in the range of 0–1208 eV were recorded in 1 eV step for each sample, followed by high resolution spectra over different element peaks in 0.1 eV steps, from which the detailed composition was calculated. Furthermore, curve-fitting was performed after a Shirley background subtraction by non-linear least square fitting using a mixed Gauss/Lorentz function [14,15]. The spectra were referenced to the C1s line at 284.8 eV. The sputter rate determined on a 30-nm thick silica (SiO_2) sample was 3.5 nm min^{-1}. The signal was collected four times for every sample. DDS-320 conductivity meter and DJS-1 conductivity electrode were used to measure the conductivity of ChCl-EG deep eutectic solvent at different temperatures.

3. RESULTS AND DISCUSSION

3.1. Electrochemical behaviors of Cr(III) ions in ChCl-EG deep eutectic solvent

Fig. 1 shows the Voltammograms recorded in ChCl-EG deep eutectic solvent with different molar ratios on glassy carbon electrode. A single oxidation peak located at 0.75 V corresponds to the oxidation of chloride (Cl^-) ions [23]. With the increase in the EG content in the ChCl-EG DES, the electrochemical window (EW) of the DES increases from 2.105 to 2.301 V. Compared to the aqueous solution (1.23 V) [24], it is apparent that the ChCl-EG DES has a wider EW. With the increase of EG content, the current of oxidation peak decreases and the potential shifts to a positive value. This phenomenon indicates that the increase of EG inhibits the oxidation of Cl^- ion in the DES [23].

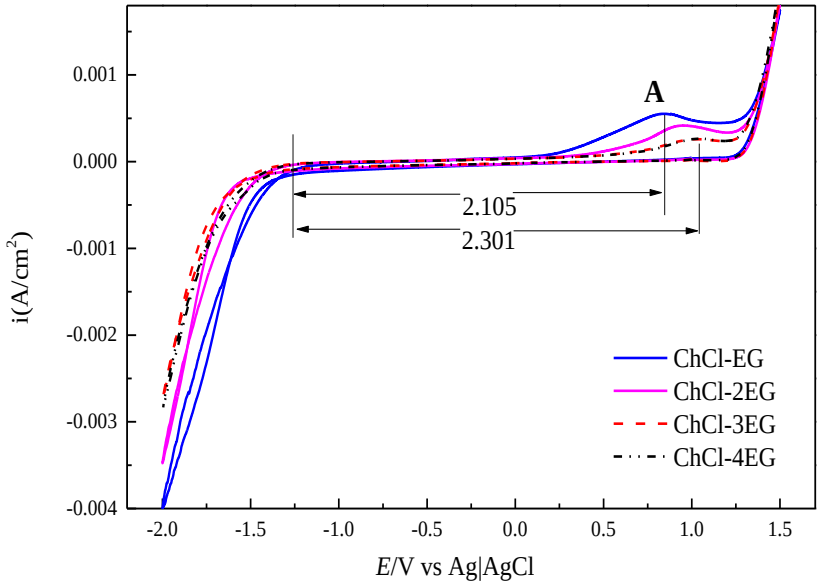

Figure 1. CV curves of ChCl-EG deep eutectic solvent with different molar ratios at the GC electrode (333 K, and the scan rate 50 mV. s^{-1})

The CV curves of Cr(III) ions electrolyte under different molar ratios are shown in Fig. 2. Clearly, when the negative sweep reaches −0.5 V, a reduction peak appears, which is labeled as "a", corresponding to Cr(III)→Cr(II) [25]. Further, a reduction peak appears when the negative sweep reaches −1.33 V, and it is labeled as "b", corresponding to Cr(II)→Cr(0) [18]. It was thus concluded that the reduction of Cr(III) ions in the ChCl-EG DES followed a two-step process. This indicates that the Cr(III) ions undergo a cathodic electrochemical reduction process in ChCl-EG DES to form a relatively stable intermediate product. Further, the formation of the divalent chromium Cr(II) compound is considered as a control step [26]. Moreover, the slower rate of reduction of divalent chromium causes the accumulation of a large amount of Cr(II) on the cathode surface. It is similar to the reduction process of Cr(III) ions in aqueous solution [27,28].

Fig. 2 also demonstrates that the peak currents of the two reduction peaks increase with the increase of the EG content. However, when the molar ratio is more than 1:3, the reduction current

decreases, which indicates that too high content of EG inhibits the two-step reduction of Cr(III) ions. Therefore, the optimum molar ratio is 1:3. Studies have also shown that the viscosity of ChCl-based DESs is closely related to the nature of HBDs [14].

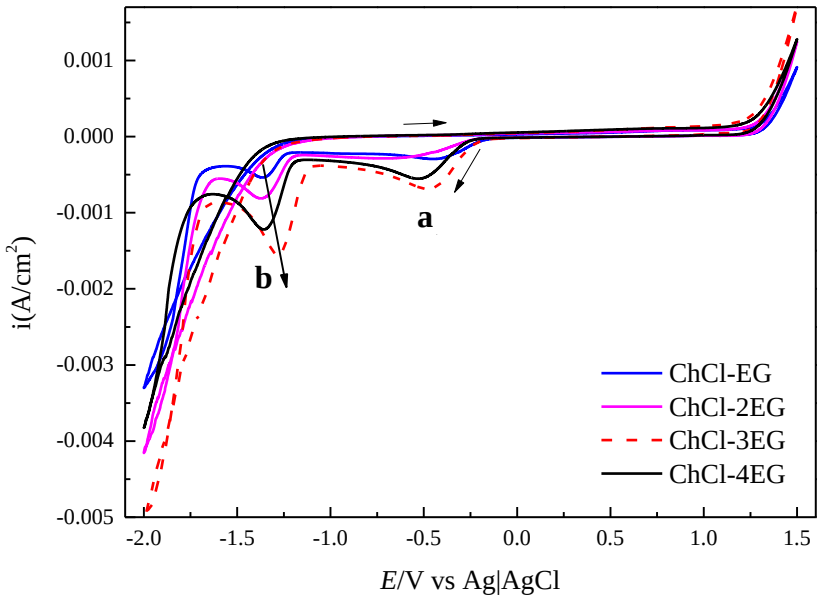

Figure 2. CV curves of Cr(III) ions in ChCl-EG deep eutectic solvents with different molar ratios at the GC electrode (333 K, and scan rate 50 mV. s^{-1})

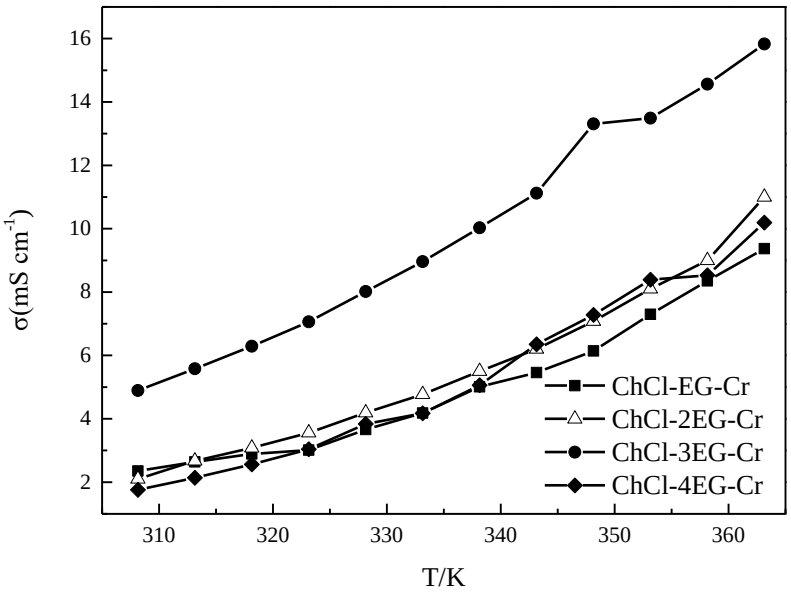

Figure 3. Conductivity curves of ChCl-EG-$CrCl_3$ under different temperatures, at molar ratios of 1:1, 1:2, 1:3, and 1:4, respectively

When the molar ratio of ChCl-EG is 1:2, 1:3, and 1:4, their viscosity is 36, 19, and 19 (temperature 20 °C), respectively [9,14]. Therefore, the ChCl-EG molar ratio coincides with the

oxidation peaks at 1:3 and 1:4. The increase in EG content significantly reduces the viscosity of the DES, resulting in increased mobility of free species and promoting the reduction of Cr(III) ions. Fig. 3 exhibits that when the mole ratio is 1:3, the highest conductivity is observed. With the increase of EG in electrolyte, the distance between ions becomes smaller and the electrostatic interaction between ions increases rapidly. When the concentration of electrolyte solution reaches a certain value, its conductivity does not increase with the increase of concentration, but decreases with the increase of concentration. Which explains that when the mole ratio is 1:3, the peak value current of reduction peak is the largest.

3.2. X-ray photoelectron spectroscopy analysis of chromium coating

The information about elements existing in the chromate coating and absorbed surface contamination can be obtained from the wide scan X-ray photoelectron spectra. Fig. 4 shows the typical XPS survey spectra of the black chromium coating obtained from ChCl-EG DES, revealing that the chromium coating on brass consists primarily of Cr, O, and C elements. Carbon has been found on sample as impurities acquired from handling the sample in air. Hydrogen could also be present, but cannot be detected by the XPS measurement [29,30].

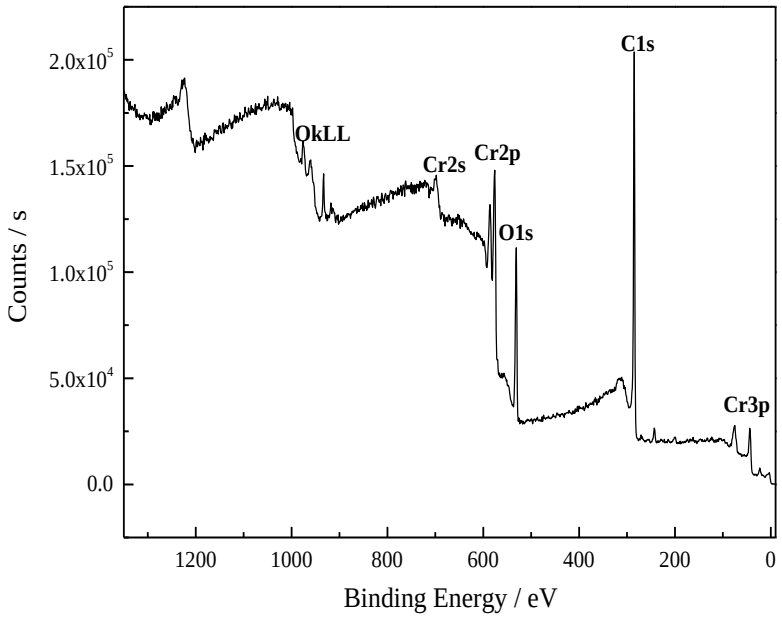

Figure 4. Typical XPS survey spectra for the chromate coating carried out on the brass surface

The results of different sputtering times on the surface of the chromium coating indicate that, when the sputtering time is 0 s, the content percentages of oxygen and chromium are 78.9 and 21.1%, respectively. In contrast, when the sputtering time is 60 s, the content percentages of oxygen and chromium are 65.8 and 34.2%, respectively. Thus the results show that after 60 s of sputtering on the sample surface, the oxygen content decreases and the chromium content increases, indicating the adsorption of water molecules on the surface of the experimental sample [16].

Fig. 5 shows the XPS narrow scanning spectra of Cr2p3/2 and Cr2p1/2 peaks of the chromium coating obtained by electrodeposition in ChCl-EG DES after Ar^+ ion bombardment for 60 s. Fig. 5 clearly demonstrates that the Cr2p peak can be deconvoluted into two peaks Cr2p3/2 and Cr2p1/2.

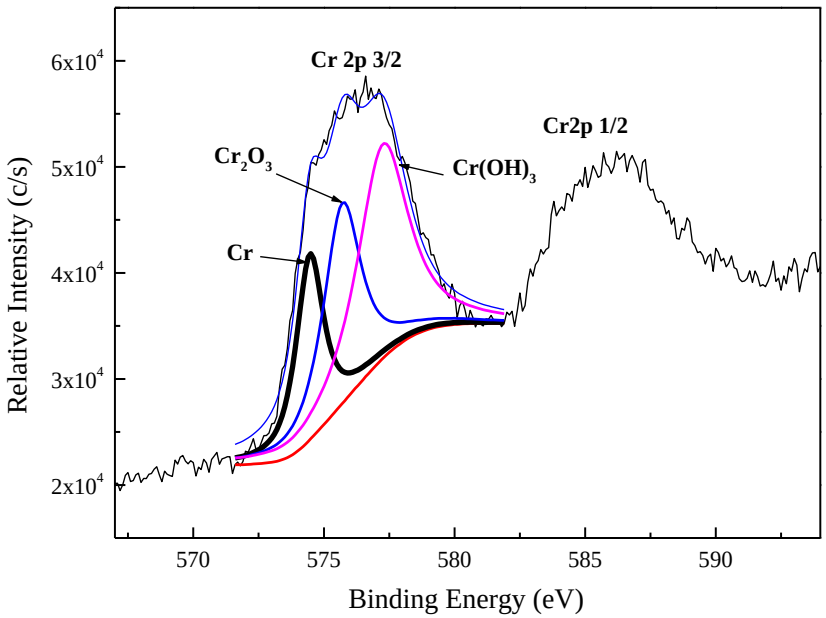

Figure 5. Narrow scanning spectra of Cr2p3/2 in the coating: the base line (Red), Cr_2O_3 (Blue curve), $Cr(OH)_3$ (Purple curve), and Cr (Black curve)

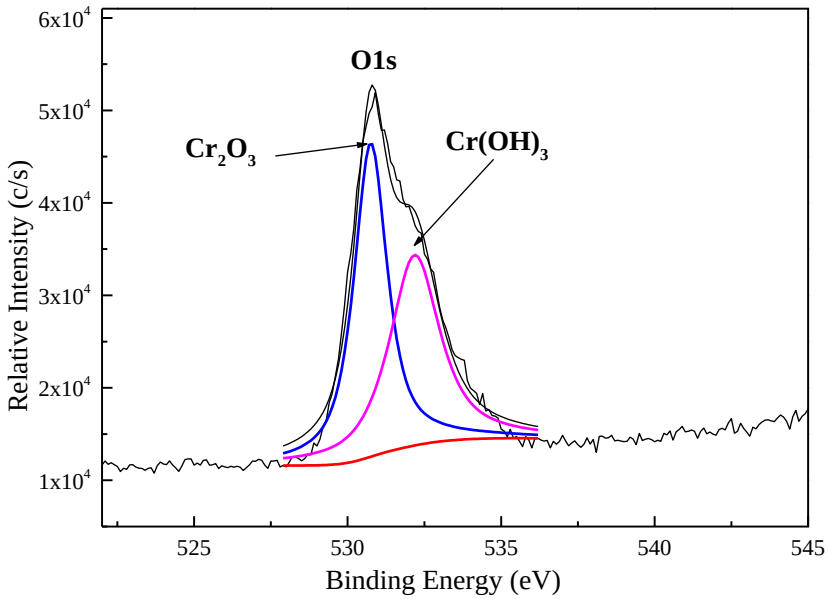

Figure 6. Narrow scan of O 1s peak in the coating: the base line (Red), Cr_2O_3 (Blue curve), and $Cr(OH)_3$ (Purple curve)

According to the results, the first sub-peak Cr2p3/2 is at 577.1 eV and the other sub-peak

Cr2p1/2 is at 586.8 eV. After fitting the Cr2p3/2 peak, three fitted peaks can be obtained with their central positions at 574.458, 575.698, and 577.248 eV, respectively [31,32]. The literature studies show that the Cr2p3/2 peak position of Cr–O bond in $Cr(OH)_3$ is 577.3 eV, which is close to the position of the third fitted peak (577.248 eV) of the plated peak, indicating that the binding state of Cr to the peak is $Cr(OH)_3$ [20,33]. Moreover, the peak position of Cr2p3/2 in Cr_2O_3 is 576.3 eV. From the numerical perspective, the binding state of Cr corresponding to the second fitting peak (575.698 eV) of Cr2p3/2 peak is close to that of Cr in Cr_2O_3, indicating that the binding state of Cr corresponding to the second fitting peak of Cr2p3/2 peak is Cr_2O_3. The peak position of elemental Cr is 574.4 eV, which corresponds to the first fitted peak in the figure.

Fig. 6 exhibits the XPS narrow scanning spectra and fitting peaks of O1s spectra. The O1s peak can be fitted into two peaks. The literature study [33] indicates that the peak at 530.77 eV is O(II) in Cr_2O_3 and the peak at 532.17 eV is O(II) in $Cr(OH)_3$.

3.3. Micro-morphology and elemental composition

Fig. 7 shows the micro-morphology and elemental composition of the black chromium coating obtained from ChCl-EG DES. Fig. 7a shows the existence of scattered cracks on the surface of the coating and a non-uniform distribution is exhibited. Elemental composition and distribution indicate that the chromium coating is mainly composed of chromium and oxygen elements, and the two elements are evenly distributed in the plating layer.

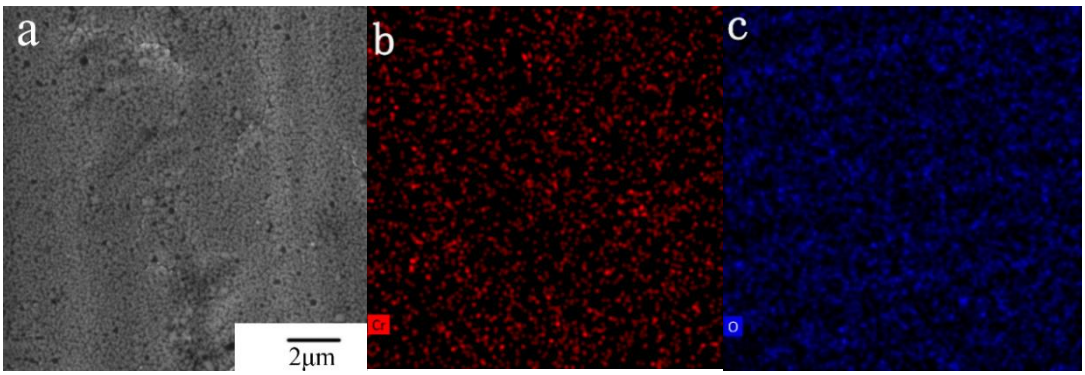

Figure 7. (a) SEM images of chromium deposit onto the surface of brass after potentiostatic deposition (−1.35 V *vs* Pt, 333 K and 30 min) from DES and (b, c) the elemental composition of the coating

4. DISCUSSION

Regarding the problem associated with the multi-step mechanism of the chromium deposition process, Vashchenko et al. [34] proposed the possibility of simultaneous transfer of three electrons. They further discussed the direct transfer of the three electrons during chromium electrodeposition from the acetic acid complex of Cr(III) without forming an intermediate. Subsequently, a multi-step reaction scheme for Cr(III) ion reduction was proposed, which is also widely accepted by most

researchers. Based on this, it is thus believed that the rate of the chromium deposition reaction depends on the concentration of the reactants that are not immediately involved in the overall reaction. Furthermore, Watson et al. [35] pointed out that it takes time for Cr(II) to be reduced to Cr(0), which leads to the accumulation of Cr(II) in the cathode diffusion layer. This accumulation makes the step of Cr(II)→Cr(0) to be the control step, and the formation of the Cr(II) polymer or oligomer species interferes with the deposition process. Therefore, if the content of Cr(II) cannot be controlled, it can lead to continuous deposition failure.

The electrodeposition of Cr(III) in aqueous solution can be divided into the following three parts:

(1) Incomplete reduction of Cr(III)

$Cr^{3+} + e^- \rightarrow Cr^{2+}$ (1)

(2) Electrodeposition of chromium metal

$Cr^{3+} + 3e^- \rightarrow Cr$ (2)

$Cr^{2+} + 2e^- \rightarrow Cr$ (3)

(3) Hydrogen evolution reaction [4]

$2H_3O^+ + 2e^- \rightarrow H_2 + 2H_2O$ (4)

$2H_2O + 2e^- \rightarrow H_2 + 2OH^-$ (5)

According to literature [6], the results of ultraviolet–visible (UV—Vis) spectroscopy of Cr(III) ion-ChCl-EG DES indicate that Cr(III) generally exists in the form of $[Cr(H_2O)_5Cl]^{2+}$, $[Cr(H_2O)_4Cl]^+$, and $[Cr(H_2O)_3Cl]$. The addition of Cl^- ions can destroy the stability of the initial chromium compound $[Cr(H_2O)_6]^{3+}$ by prolonging the Cr–H_2O bond [2,5]. In the $[Cr(H_2O)_6]^{3+}$ complex, the Cr–H_2O bond length was 1.99 Å. The elongation of Cr–H_2O bond due to the existence of Cl^- ions in Cr-complex is beneficial to the fracture of d-orbital of Cr^{3+} and promotes the formation of intermediates during the Cr(III) reduction reaction [40].

However, the chromium chloride used in the experiment has six crystal waters, and a part of Cr(III) remains in the DES in the form of $[Cr(H_2O)_6]^{3+}$ [36]. According to the valence bond theory, $[Cr(H_2O)_6]^{3+}$ is an internal orbital coordination compound. During the electrodeposition process, electrons on the cathode cannot enter the inner orbit to replace H_2O because there is no remaining d-orbital to immediately participate in the reaction [26]. This makes $[Cr(H_2O)_6]^{3+}$ extremely stable, and it can only be reduced when its potential is more negative than the water reduction potential. This results in hydrogen evolution and a higher pH on the surface of the electrode near the electrode layer than in the bulk electrolyte [37]. When pH > 4, hydration $[Cr(H_2O)_6]^{3+}$ undergoes a hydroxyl bridged oxygen, which causes Cr(III) to polymerize into a long-chain polymerized complex gel [38]. The colloidal precipitate is easily adsorbed on the cathode surface, preventing further reduction of chromium ions. Furthermore, an increase in the pH near the cathode causes the formation of chromium hydroxide on the substrate surface, resulting in the appearance of a black coating [39]. Noteworthy, adsorption of poorly soluble chromium hydroxide on the electrode surface also blocks the local current density of chromium reduction [40].

Angulo et al. [41] also emphasized that some chromium hydroxide compounds are involved in the multi-step electrochemical reaction of Cr(III) electroreduction. Danilov et al. [40] believed that the presence of hydroxide ions is one of the causes of the decrease in the efficiency of electrodeposition

current. The increase in pH of the electrode surface is the direct cause of OH^- production, thus generating hydroxide in the process of electrodeposition. This indicates that the water molecules in the first ligand sphere of the complex chromium ion are first replaced by an OH^- group after complex changed from Cr(III) to Cr(II), as shown in equations (6) and (7). Then, transformation into Cr(0) complex occurs, as shown in equation (8). Finally, chromium coating is formed, as shown in equation (9).

$$[Cr(III)(H_2O)_5Cl]^{2+} + e^- \rightarrow [Cr(II)(H_2O)_5Cl]^+ \quad (6)$$

$$[Cr(II)(H_2O)_5Cl]^+ \rightarrow [Cr(II)(H_2O)_4(OH)Cl] + H^+ \text{ or}$$

$$[Cr(II)(H_2O)_5Cl]^+ + OH^- \rightarrow [Cr(II)(H_2O)_4(OH)Cl] + H_2O \quad (7)$$

$$[Cr(II)(H_2O)_4(OH)Cl] + 2e^- \rightarrow [Cr(0)(H_2O)_4(OH)Cl]^{2-} \quad (8)$$

$$[Cr(0)(H_2O)_4(OH)Cl]^{2-} \rightarrow Cr^0 + 4H_2O + OH^- + Cl^- \quad (9)$$

The reduction mechanism of chromium electrodeposition in ChCl-EG DES was proposed as revealed in equations (6) to (9). Moreover, the XPS results show that the coating is composed of Cr(0), Cr_2O_3, and $Cr(OH)_3$. A small amount of OH^- appears in the IL, and OH^- then combines with Cr^{3+} to form $Cr(OH)_3$, which is further dehydrated to produce Cr_2O_3.

5. CONCLUSION

Black chromium coating with some cracks was prepared in choline chloride-ethylene glycol (ChCl-EG) deep eutectic solvent via electrodeposition method. With the increase in the content of EG, the electrochemical window of ionic liquid increased from 2.105 to 2.301 V, and the oxidation of chloride in ionic liquid was inhibited. The reduction of Cr(III) ions followed a two-step process: Cr(III)→Cr(II)→Cr(0). The chromium coating was found to consist of Cr, $Cr(OH)_3$, and Cr_2O_3. Furthermore, a systemic reaction process was proposed to explain the reduction mechanism of chromium electrodeposition in ChCl-EG deep eutectic solvent.

ACKNOWLEDGEMENTS
This work was supported by the project of Liaoning Shenyang National Research Center for Materials Science (Projects: 2019JH3/30100021). We also like to express our gratitude to the anonymous reviewers of this paper for their criticisms and suggestions that contributed to improve our work.

References

1. N.V. Mandich and D.L. Snyder (Eds.), Modern Electroplating, Fifth Edition. (2011) Wiley, Canada.
2. T. Derabla, A.M. Affoune and M.L. Chelaghmia, *Surf. Engin. Appl. Electrochem.,* 55 (2019) 304.
3. Z. Abdel Hamid, I.M. Ghayad and K.M. Ibrahim, *Surf. Interface Anal.*, 37 (2005) 573.
4. V.V. Kuznetsov, E.G. Vinokurov and V.N. Kudryavtsev, *Russ. J. Electrochem.*, 37 (2001) 699.
5. V.A. Safonov, L.N. Vykhodtseva, Y.M. Polukarov, O.V. Safonova, G. Smolentsev, M. Sikora, S.G. Eeckhout and P. Glatzel, *J. Phys. Chem. B,* 110 (2006) 23192.
6. L. Li, S. Niu, Z. Shi, H. Wu, W. Zhu, J. Jin, Y. Chi and Y. Xing, *J. Inorg Organomet Polym.*, 21 (2010) 15.
7. A.P. Abbott, D. Boothby, G. Capper, D.L. Davies and R.K. Rasheed, *J. Am. Chem. Soc.*, 126

(2004) 9142.
8. R.K. Choudhary, V. Kain and R.C. Hubli, *Surf. Eng*., 30 (2014) 562.
9. Q. Zhang, K.D.O. Vigier, R. Sébastien and F. Jérôme, *Chem. Soc. Rev.,* 41 (2012) 7108.
10. M. Amiri, C. Boissy, C. Gottardo and A. Chen, *J. Appl. Electrochem.*, 48 (2018) 901.
11. Q.Q. Zhang, Q. Wang and S.J. Zhang , *Chemphyschem,* 17 (2016) 335.
12. A.P. Abbott, G. Capper, D.L. Davies, R.K. Rasheed and V. Tambyrajah, *Chem. Commun.*, 9 (2003) 70.
13. F. Gan, K. Chen, N. Li, Y. Wang, S. yi and X. He, *Ionics,* 25 (2019) 4243.
14. A.P. Abbott, D. Boothby, G. Capper, D.L. Davies and R.K. Rasheed, *J. Am. Chem. Soc*., 126 (2004) 9142–9147.
15. Q. Li, J. Jiang, G. Li, W. Zhao, X. Zhao and T. Mu, *Sci. China Chem*., 59 (2016) 571.
16. S. Survilienė, S. Eugénio and R. Vilar, *J. Appl. Electrochem*., 41 (2011) 107.
17. X. He, B. Hou, C. Li, Q. Zhu, Y. Jiang and L. Wu, *Electrochim. Acta*, 130 (2014) 245.
18. X. He, Q. Zhu, B. Hou, C. Li, Y. Jiang, C. Zhang and L. Wu, *Surf. Coat. Technol*., 262 (2015) 148.
19. J. Maharaja, M. Raja and S. Mohan, *Surf. Eng*., 30 (2014) 722.
20. Rudolf Holze. Electrodeposition from ionic liquids. F. Endres, A. P. Abbott, and D. R. MacFarlane (Eds). (2008) WILEY-VCH, Weinheim.
21. S. Eugénio, C.M. Rangel, R. Vilar and S. Quaresma, *Electrochim. Acta,* 56 (2011)10347.
22. A.P. Abbott, G. Capper, D.L. Davies, R.K. Rasheed, J. Archer and C. John, *Trans. Inst. Met. Finish*, 82 (2004) 14.
23. L. Anicai, A. Petica, S. Costovici, P. Prioteasa and V. Teodor, *Electrochim. Acta*, 114 (2013) 868.
24. Y. Zhang, R. Ye, D. Henkensmeier, R. Hempelmann and R. Chen, *Electrochim. Acta*, 263 (2018) 47.
25. M. Paunovic, M. Schlesinger (Eds.), Fundamentals of Electrochemical Deposition, second ed., (2006) Wiley-Interscience, Hoboken, New Jersey.
26. A. Watson, A.M.H. Anderson, M.R. El-Sharif and C.U. Chisholm, *Trans. Inst. Met. Finish*, 69 (1991) 26.
27. Y. Sheasha and D. Yücel, *ChemElectroChem*, 4 (2017) 1390.
28. S.P. Jiang and X. Chen, *ChemInform*, 45 (2014).
29. S Men and J Jiang, *J. Appl. Spectrosc*., 85 (2018) 55.
30. C.C.S. Dias, Q.B.G. Mello, L. Richard, D.S.M.G. Carlos and V.M.G. Adeodato, *Environ. Sci. Pollut. Res.*, 26 (2019) 28470.
31. E. Fernández-Díaz, A.B. Espinoza-Martinez, A. Flores-Pacheco, R. Ramírez-Bon, S.J. Castillo and R. Ochoa-Landin, *J. Elec. Materi.*, 48 (2019) 3405.
32. J. Sun, G.C. Qi, Y. Tan and C.Q. An, *Surf. Interface Anal.*, 41 (2009) 449.
33. V. Maurice, W.P. Yang and P. Marcus, *J. Electrochem. Soc*., 141 (1994) 3016.
34. S.V. Vashchenko, L.N. Solodkova and Z.A. Solov'eva, *Russ. J. Electrochem*., 36 (2000) 947.
35. A. Watson, A.M.H. Anderson, M.R. el-Sharif and C.U. Chisholm, *Trans. Inst. Met. Finish*, 69 (1991) 26.
36. P.J. Elving and B. Zemel, *J. Am. Chem. Soc*., 79 (1957) 1281.
37. V.S. Protsenko, L.S. Bobrova, D.E. Golubtsov, S.A. Korniy and F.I. Danilov, *Russ. J. Appl. Chem.*, 91 (2018) 1106.
38. N.V. Mandich, *Chemistry Cheminform*., 28(1997).
39. X. Zhang and J.A. Koropchak, *Appl. Spectrosc*., 56 (2002) 1152.
40. F.I. Danilov and V.S. Protsenko, *Prot. Met.*, 37 (2001) 223.
41. A. Angulo, J.A. Merchán and M. Molina, *J. Histochem. Cytochem*., 42 (1994) 393.